

# MODERN PATHOLOGY

# ABSTRACTS

CARDIOVASCULAR PATHOLOGY  
(300-316)



USCAP 109TH ANNUAL MEETING  
**2020**  
EYES ON YOU

FEBRUARY 29-MARCH 5, 2020

LOS ANGELES CONVENTION CENTER  
LOS ANGELES, CALIFORNIA

**EDUCATION COMMITTEE**

**Jason L. Hornick**, Chair  
**Rhonda K. Yantiss**, Chair, Abstract Review Board  
 and Assignment Committee  
**Laura W. Lamps**, Chair, CME Subcommittee  
**Steven D. Billings**, Interactive Microscopy Subcommittee  
**Raja R. Seethala**, Short Course Coordinator  
**Ilan Weinreb**, Subcommittee for Unique Live Course Offerings  
**David B. Kaminsky** (Ex-Officio)  
**Zubair Baloch**  
**Daniel Brat**  
**Ashley M. Cimino-Mathews**  
**James R. Cook**  
**Sarah Dry**

**William C. Faquin**  
**Yuri Fedoriw**  
**Karen Fritchie**  
**Lakshmi Priya Kunju**  
**Anna Marie Mulligan**  
**Rish K. Pai**  
**David Papke**, Pathologist-in-Training  
**Vinita Parkash**  
**Carlos Parra-Herran**  
**Anil V. Parwani**  
**Rajiv M. Patel**  
**Deepa T. Patil**  
**Lynette M. Sholl**  
**Nicholas A. Zoumberos**, Pathologist-in-Training

**ABSTRACT REVIEW BOARD**

**Benjamin Adam**  
**Narasimhan Agaram**  
**Rouba Ali-Fehmi**  
**Ghassan Allo**  
**Isabel Alvarado-Cabrero**  
**Catalina Amador**  
**Roberto Barrios**  
**Rohit Bhargava**  
**Jennifer Boland**  
**Alain Borczuk**  
**Elena Brachtel**  
**Marilyn Bui**  
**Eric Burks**  
**Shelley Caltharp**  
**Barbara Centeno**  
**Joanna Chan**  
**Jennifer Chapman**  
**Hui Chen**  
**Beth Clark**  
**James Conner**  
**Alejandro Contreras**  
**Claudiu Cotta**  
**Jennifer Cotter**  
**Sonika Dahiya**  
**Farbod Darvishian**  
**Jessica Davis**  
**Heather Dawson**  
**Elizabeth Demicco**  
**Katie Dennis**  
**Anand Dighe**  
**Suzanne Dintzis**  
**Michelle Downes**  
**Andrew Evans**  
**Michael Feely**  
**Dennis Firchau**  
**Gregory Fishbein**  
**Andrew Folpe**  
**Larissa Furtado**

**Billie Fyfe-Kirschner**  
**Giovanna Giannico**  
**Anthony Gill**  
**Paula Ginter**  
**Tamara Giorgadze**  
**Purva Gopal**  
**Anuradha Gopalan**  
**Abha Goyal**  
**Rondell Graham**  
**Alejandro Gru**  
**Nilesh Gupta**  
**Mamta Gupta**  
**Gillian Hale**  
**Suntrea Hammer**  
**Malini Harigopal**  
**Douglas Hartman**  
**John Higgins**  
**Mai Hoang**  
**Mojgan Hosseini**  
**Aaron Huber**  
**Peter Illei**  
**Doina Ivan**  
**Wei Jiang**  
**Vickie Jo**  
**Kirk Jones**  
**Neerja Kambham**  
**Chiah Sui Kao**  
**Dipti Karamchandani**  
**Darcy Kerr**  
**Ashraf Khan**  
**Francesca Khani**  
**Rebecca King**  
**Veronica Klepeis**  
**Gregor Krings**  
**Asangi Kumarapeli**  
**Alvaro Laga**  
**Steven Lagana**  
**Keith Lai**

**Michael Lee**  
**Cheng-Han Lee**  
**Madelyn Lev**  
**Zaibo Li**  
**Faqian Li**  
**Ying Li**  
**Haiyan Liu**  
**Xiuli Liu**  
**Yen-Chun Liu**  
**Lesley Lomo**  
**Tamara Lotan**  
**Anthony Magliocco**  
**Kruti Maniar**  
**Emily Mason**  
**David McClintock**  
**Bruce McManus**  
**David Meredith**  
**Anne Mills**  
**Neda Moatamed**  
**Sara Monaco**  
**Atis Muehlenbachs**  
**Bitu Naini**  
**Dianna Ng**  
**Tony Ng**  
**Michiya Nishino**  
**Scott Owens**  
**Jacqueline Parai**  
**Yan Peng**  
**Manju Prasad**  
**Peter Pytel**  
**Stephen Raab**  
**Joseph Rabban**  
**Stanley Radio**  
**Emad Rakha**  
**Preetha Ramalingam**  
**Priya Rao**  
**Robyn Reed**  
**Michelle Reid**

**Natasha Rektman**  
**Jordan Reynolds**  
**Michael Rivera**  
**Andres Roma**  
**Avi Rosenberg**  
**Esther Rossi**  
**Peter Sadow**  
**Steven Salvatore**  
**Souzan Sanati**  
**Anjali Saqi**  
**Jeanne Shen**  
**Jiaqi Shi**  
**Gabriel Sica**  
**Alexa Siddon**  
**Deepika Sirohi**  
**Kalliopi Siziopikou**  
**Sara Szabo**  
**Julie Teruya-Feldstein**  
**Khin Thway**  
**Rashmi Tondon**  
**Jose Torrealba**  
**Andrew Turk**  
**Evi Vakiani**  
**Christopher VandenBussche**  
**Paul VanderLaan**  
**Olga Weinberg**  
**Sara Wobker**  
**Shaofeng Yan**  
**Anjana Yeldandi**  
**Akihiko Yoshida**  
**Gloria Young**  
**Minghao Zhong**  
**Yaolin Zhou**  
**Hongfa Zhu**  
**Debra Zynger**

To cite abstracts in this publication, please use the following format: **Author A, Author B, Author C, et al. Abstract title (abs#). In "File Title." *Modern Pathology* 2020; 33 (suppl 2): page#**

### 300 Efficacy of Bilateral Temporal Artery Biopsies and Sectioning of the Entire Block of Tissue for the Diagnosis of Temporal Arteritis

Adrian Agostino<sup>1</sup>, Paula Blanco<sup>2</sup>, James Farmer<sup>3</sup>, John Veinot<sup>4</sup>, Vidhya Nair<sup>1</sup>  
<sup>1</sup>University of Ottawa, Ottawa, ON, <sup>2</sup>Ottawa, ON, <sup>3</sup>Queen's University, Kingston, and the University of Ottawa, Ottawa, ON, <sup>4</sup>Ottawa Hospital, Ottawa, ON

**Disclosures:** Adrian Agostino: None; Paula Blanco: None; James Farmer: None; John Veinot: None; Vidhya Nair: None

**Background:** It is important to establish the diagnosis of temporal arteritis because the disease is treatable; treatment may prevent blindness and even death. An arterial biopsy showing giant cell arteritis establishes the diagnosis. There is variation amongst centers in the type of biopsies (unilateral or bilateral) performed and also the processing of these specimens. The objective of this retrospective study is to determine a) the efficacy of bilateral temporal artery biopsies and b) the efficacy of sectioning the entire block in detecting the pathologic changes of giant cell arteritis.

**Design:** This will be a single center retrospective study. The pathology reports of consecutive temporal artery biopsy specimens received in the department of pathology, University of Ottawa from July 2010 to July 2019 (9 years) were reviewed. The Temporal artery biopsies that are positive for arteritis were noted. A note was made if the temporal biopsies were unilateral or bilateral. Slides from the positive cases were retrieved and reviewed. A note was made for which level the artery biopsy was positive.

**Results:** The number of biopsies that were positive for Temporal Arteritis was 203. Unilateral biopsies were performed in 18 cases. In 185 cases, where bilateral biopsies were performed, the biopsies were positive on only one side in 26 cases (14%). Due to time constraints, only slides from positive cases in the last two years were examined. When the levels were examined from 101 positive biopsies, we had the following results: 70 cases were positive on level 1, 23 cases on level 3, 3 cases on level 5, 3 cases on level 7, 1 case on level 9 and 1 case on level 13. In 96 cases (95%), the cases were positive when initial 5 levels were examined.

**Conclusions:** The results of this study indicate that performing a bilateral simultaneous temporal artery biopsy improves the diagnostic yield in at least 14% of cases of giant cell arteritis. Thus, in patients in whom only one artery is biopsied, there is a probability of missing the correct diagnosis. The consequences of both delayed diagnosis and treatment of individuals who have giant cell arteritis are of such potential severity that consideration should always be given to performing bilateral temporal artery biopsies in patients suspected of having the disease. Although 95% are diagnosed on 5 levels, serious consideration should be given to more extensive sectioning as the consequences of missing 5% can mean total loss of vision.

### 301 KRAS Mutational Status in Papillary Fibroelastomas is Not Predictive of Tumor Growth Rate or Clinical Behavior

Melanie Bois<sup>1</sup>, Ahmed Sorour<sup>1</sup>, Reto Kurmann<sup>1</sup>, Edward El-Am<sup>2</sup>, Christopher Scott<sup>1</sup>, Dragana Milosevic<sup>1</sup>, Benjamin Kipp<sup>1</sup>, Kyle Klarich<sup>1</sup>, Joseph Maleszewski<sup>1</sup>  
<sup>1</sup>Mayo Clinic, Rochester, MN, <sup>2</sup>Mayo Clinic, Indianapolis, IN

**Disclosures:** Melanie Bois: None; Ahmed Sorour: None; Reto Kurmann: None; Edward El-Am: None; Christopher Scott: None; Dragana Milosevic: None; Joseph Maleszewski: None

**Background:** Papillary fibroelastomas (PFEs) are benign endocardial growths that are most commonly encountered on the cardiac valves. Despite their histologic benignity, they may be associated with serious morbidity including transient ischemic attack, cerebral infarction, or myocardial infarction. Recently, a subset of PFEs have been shown to harbor driver mutations in *KRAS*, though whether or not these mutations impart clinical significance has yet to be determined.

**Design:** Institutional archives were queried for cases of surgically excised PFE (1995-2018). Cases were reviewed for confirmation of diagnosis. Relevant clinical information was abstracted from the medical record and echocardiography databases. Formalin-fixed paraffin-embedded tissue was microdissected for tumor isolation. Extracted DNA underwent droplet digital polymerase chain reaction analysis of the most common *KRAS* mutations (codons 12, 13 and 61). Borderline cases were repeated. Fractional abundance of mutant DNA >1% and >14 copies detected was considered positive.

**Results:** 270 patients (166 women) were identified in accordance with aforementioned criteria. Median age at the time of excision was 65 years (interquartile range 55-73). 237 (88%) had residual analyzable material for molecular testing. Of those, 35 (14.8%) harbored *KRAS* mutations (27 in codons 12/13; 8 in codon 61). Mutations were mutual exclusive. *KRAS* mutation status did not influence PFE growth rate (p=0.70), PFE size (p=0.12), or likelihood of embolization (peripheral, p=0.11 or central nervous system, p=0.68), and was not predicative of prior radiation history (p=0.22), malignancy (p=0.18), or cardiac surgery (p=0.63).

**Conclusions:** While the finding of *KRAS* mutations in a subset of PFEs has provided valuable information regarding the etiologic underpinnings of these lesions, the significance of these mutations has not been extensively studied. *KRAS*-mutated PFEs do not appear to differ from their wild-type counterparts with respect to tumor growth rate. Furthermore, in a sizeable cohort of PFEs, there was no

demonstrated difference in presentation/clinical behavior between the mutant and wild-type tumors. Routine testing of PFEs for KRAS mutations does not appear to be of clinical import at this time.

### 302 Detecting Cardiac Transplant Antibody Mediated Rejection by Artificial Intelligence: A Novel Deep Learning Approach

Richard Davis<sup>1</sup>, John Carney<sup>2</sup>, Louis Dibernardo<sup>2</sup>, Elizabeth Pavlisko<sup>2</sup>, Matthew Glass<sup>1</sup>, Carolyn Glass<sup>2</sup>  
<sup>1</sup>Duke University, Durham, NC, <sup>2</sup>Duke University Medical Center, Durham, NC

**Disclosures:** Richard Davis: None; John Carney: None; Elizabeth Pavlisko: None; Matthew Glass: None; Carolyn Glass: None

**Background:** Pathologic antibody mediated rejection (pAMR) remains a major driver of graft failure in cardiac transplant patients. The biopsy remains the primary diagnostic tool but challenges remain in distinguishing the histologic component (pAMR-H) defined by 1) intravascular macrophage accumulation in capillaries and 2) activated endothelial cells that narrow or occlude the vascular lumen. Frequently, pAMR-H is difficult to distinguish from acute cellular rejection (ACR) and healing injury. We determined if a machine learning algorithm (MDL) can distinguish pAMR-H from normal myocardium, healing injury and ACR.

**Design:** A total of 4000 annotations (1000 regions of normal, 1000 pAMR-H, 1000 healing injury and 1000 ACR) were made from 150 hematoxylin and eosin slides scanned using a Leica Aperio AT2 digital whole slide scanner at 40X magnification. All regions of pAMR-H were annotated from patients confirmed with pAMR2 (>50% positive C4d immunofluorescence and/or >10% CD68 positive intravascular macrophages). A four-layered annotation system of histologic primitives was used to divide annotations into normal, healing injury, pAMR-H and ACR regions of interest using Leica ImageScope Software. A convolutional neural network utilizing transfer learning was trained to identify the different classes. The convolutional base of the VGG16 network with frozen "Imagenet" weights was used to train our fully connected layer with 256 hidden units. After initially training our fully connected layer, the last few layers of the convolutional base were unlocked and trained concurrently with our dense layer to fine-tune the network.

**Results:** The MDL algorithm showed 96% overall validation accuracy which included all groups. pAMR-H was then distinguished from normal myocardium, healing injury and ACR with 96%, 99% and 97% accuracy, respectively. For the human diagnosis, inter-institutional accuracy between 3 cardiac pathologists was mean 88% for pAMR-H. There was even higher variability between pathologists for the presence of acute cellular rejection admixed with pAMR-H (mean accuracy 65%) and the presence of healing injury (mean accuracy 70%).

**Conclusions:** Our MDL algorithm can reach, and possibly surpass, acceptable performance of current diagnostic standards in identifying pAMR-H. To our knowledge this is the first study that provides evidence that a learning algorithm can be taught and validated to diagnose pAMR-H in cardiac transplant patients. Future studies should include multi-institutional validation.

### 303 Biopsy Proven Myocarditis: Current Perspectives on Viral Etiopathogenesis and Diagnostic Role of Cardiac Magnetic Resonance

Monica De Gaspari<sup>1</sup>, Stefania Rizzo<sup>2</sup>, Elisa Carturan<sup>2</sup>, Gaetano Thiene<sup>2</sup>, Martina Perazzolo Marra<sup>1</sup>, Cristina Basso<sup>3</sup>  
<sup>1</sup>University of Padua, Padua, Italy, <sup>2</sup>University of Padua, Padova, Italy, <sup>3</sup>University of Padua Medical School, Padova, Italy

**Disclosures:** Monica De Gaspari: None; Stefania Rizzo: None; Elisa Carturan: None; Gaetano Thiene: None; Martina Perazzolo Marra: None; Cristina Basso: None

**Background:** Endomyocardial biopsy (EMB) is the diagnostic gold standard for myocarditis. Cardiac magnetic resonance (CMR) is useful for tissue characterization but only EMB allows to define its etiopathogenesis. Our aim was to assess a new histopathological classification and the current etiopathogenesis of myocarditis and to validate the diagnostic role of CMR.

**Design:** Consecutive EMBs collected in the time interval 2008-2018 with a diagnosis of myocarditis and dilated cardiomyopathy (DCM) were reviewed. Timing of EMB (symptoms onset-EMB), clinical presentation, CMR, histological, immunohistological and molecular data were collected. EMB subgroups included active myocarditis (AM), chronic active myocarditis (CAM), chronic myocarditis (CM), inflammatory cardiomyopathy (ICM) and DCM. The viral data were compared with those collected in the late 90ies at our center (120 myocarditis, 26% virus positive, 12.5% enteroviral-EV positive).

**Results:** Among 602 consecutive EMBs, 406 were myocarditis (67%) and 196 DCM (33%). In the former, 124 were AM (30%), 92 CAM (23%), 27 CM (7%), 153 ICM (38%). Fifty-seven (14%) myocarditis and 33 (17%) DCM were virus positive. Parvovirus-B19 (PVB19) was the most prevalent virus in myocarditis (47%), followed by Cytomegalovirus (9%), Epstein Barr virus and Human Herpes virus 6 (7% each) with 16% multiple viruses. Interestingly, PVB19 was also detected in DCM (64% of virus positive DCM) for a total of 55 PVB19 positive EMB. However, a number of PVB19 copies >500 was found only in 25% of cases. AM was diagnosed in 42% of cases with EMB timing ≤ 7 days and in 38% with EMB timing 8 days-2 weeks; DCM was diagnosed in 35% of cases with EMB timing either 2 weeks-3 months or >3 months. In 108 patients who also underwent CMR, the EMB diagnosis of AM was significantly associated with findings compatible with

myocarditis according to Lake Louis criteria ( $p < 0.01$ ); and non-specific CMR findings were associated with an EMB diagnosis of DCM ( $p < 0.01$ ). No correlation was found between viral etiology and CMR features.

**Conclusions:** A viral etiology is currently found only in 14% of myocarditis diagnosed by EMB. This change can be attributed to the use of more sensitive molecular techniques and to EMB timing. PVB19 is the most common virus and its causal role remains controversial in the absence of quantitative data. The significant association between EMB and CMR findings in the setting of AM and DCM confirms the diagnostic role of CMR.

**304 Small Vessel Disease and Myocardial Fibrosis in Hypertrophic Cardiomyopathy: Who Comes First?**

Monica De Gaspari<sup>1</sup>, Stefania Rizzo<sup>2</sup>, Gaetano Thiene<sup>2</sup>, Cristina Basso<sup>3</sup>

<sup>1</sup>University of Padua, Padua, Italy, <sup>2</sup>University of Padua, Padova, Italy, <sup>3</sup>University of Padua Medical School, Padova, Italy

**Disclosures:** Monica De Gaspari: None; Stefania Rizzo: None; Gaetano Thiene: None; Cristina Basso: None

**Background:** Hypertrophic cardiomyopathy (HCM), an inherited myocardial disease mostly due to mutations of sarcomeric genes, is characterized by histologic changes affecting not only the cardiac myocytes but also the interstitium and microcirculation. Replacement-type fibrosis can account for either electrical instability at risk of sudden death (SD) or evolution towards end-stage heart failure (HF). Although imaging and pathology studies have demonstrated the existence of small vessel disease (SVD) in HCM, the relationship between SVD and fibrosis remains unclear and a comparison of SD-HCM and HF-HCM in terms of fibrosis and SVD is still missing.

**Design:** Macroscopic detection of scars and histological assessment of fibrosis (presence, type and site) and SVD (semi-quantitative score 0-4) were performed in HCM hearts coming from either cardiac transplantation (10 cases, mean age 52 yrs, 40% males) due to HF or autopsy due to SD in the young (30 cases, mean age 23 yrs, 83% males). As controls, 20 left ventricular apical samples for mechanical assistance device in chronic ischemic heart disease (IHD) were used.

**Results:** Replacement-type fibrosis was detected in 17 SD cases (57%) and in all HF cases (100%). Scar was transmural in all but one HF cases (90%) and never in SD cases. In the SD subgroup, patients with replacement-type fibrosis showed statistically significant higher values in terms of age, absolute and % septal thickness increase, SVD frequency, SVD max score (all  $p < 0.05$ ). Presence of SVD did not show significant differences among SD, HF and IHD cases (73%, 100% and 95%, respectively). However, SVD score was significantly different when comparing HF and SD-HCM (2.4 vs 1.18), HF-HCM and IHD (2.4 vs 1.95), and SD-HCM and IHD (1.18 vs 1.95). Noteworthy, SVD mean score was higher in fibrosis vs no fibrosis area in both HF (3.4 vs 1.4) and SD (1.4 vs 0.8) HCM hearts (all  $p < 0.05$ ).

**Conclusions:** Replacement-type fibrosis is a constant feature in HF-HCM, at difference from SD-HCM where is present in about half of cases. The presence of fibrosis is related to age, myocardial mass and wall thickness. Although SVD is present in all HCM hearts, a higher score is observed in HF cases, in HCM with replacement-type fibrosis and in areas with fibrosis compared to those without. The almost constant finding of SVD also in IHD suggests that structural changes of the microcirculation can occur also secondarily to fibrotic remodeling.

**305 Prevalence and Clinicopathological Phenotype of Cardiomyopathy Caused by Inborn Errors of Energy Metabolism in End-Stage Heart Failure Adult Patients Undergoing Cardiac Transplant**

Carla Giordano<sup>1</sup>, Elena Perli<sup>2</sup>, Annalinda Pisano<sup>2</sup>, Maria Gemma Pignataro<sup>2</sup>, Bruna Cerbelli<sup>2</sup>, Giulia d'Amati<sup>3</sup>

<sup>1</sup>Rome, Italy, <sup>2</sup>Sapienza, University of Rome, Rome, Italy, <sup>3</sup>Sapienza, University of Rome, Roma, Italy

**Disclosures:** Carla Giordano: None; Elena Perli: None

**Background:** Inherited disorders of energy metabolism are a broad spectrum of genetic disease characterized by impaired synthesis and/or use of energy substrates. Cardiomyopathy may be the unique or prevalent manifestation of the disease and may be severe enough to cause heart failure.

**Design:** A total of 110 hearts, consecutively explanted at the Department of Cardiac Surgery of San Camillo Hospital of Rome over a 6-years period, were retrospectively reviewed to assess the prevalence and clinicopathological phenotype of metabolic cardiomyopathy in adult patients with end-stage heart failure undergoing cardiac transplant (CT).

**Results:** Cardiomyopathy due to inherited disorders of energy metabolism was observed in 4 out of 110 patients (3,63%). Clinical data are reported in Table 1. In three patients (Pt1-3), skeletal muscle biopsy, performed before cardiac transplant because of a mild myopathy, suggested the diagnosis. In one patient (Pt4) analysis of explanted heart pointed to the specific etiology. All diagnoses were confirmed by genetic analysis.

At gross examination massive, symmetric, biventricular hypertrophy (mean±SD heart weight 465±55,76) was the most frequent cardiac phenotype (Pt1-3;75%). One patient (Pt4) presented with biventricular dilation associated with multiple foci of myocardial fibro-adipose replacement. At histology the more characteristic finding was the extensive cytoplasmic vacuolation of cardiac myocytes (100%). Immunohistochemistry with antibodies to lysosomal-associated membrane protein 2 (LAMP2) showed discrete clusters of either stained or unstained cardiac myocytes, consistent with a status of female carrier of Danon disease in one patient (Pt3). A large prevalence of cytochrome c oxidase (COX)-deficient cardiac myocytes on frozen sections demonstrated mitochondrial dysfunction in two patients (Pt2 and Pt4), confirmed by biochemical respiratory chain analysis of cardiac homogenate. Ultrastructural analysis revealed glycogen accumulation (Pt1), massive mitochondrial proliferation (Pt 2 and Pt4) and accumulation of autophagic vacuoles (Pt3).

I	Sex	Age at diagnosis	Age at CT	Cardiac phenotype	Extracardiac symptoms	Diagnosis
Pt1	M	19	45	HCM	Mild myopathy	Glycogenosis type IV
Pt2	M	16	20	HCM	Mild myopathy and hearing loss	Mitochondrial disease
Pt3	F	22	23	HCM, pre-excitation	Mild mental retardation and myopathy	Danon disease
Pt4	F	23	23	DCM	Mild non progressive cerebellar ataxia	Mitochondrial disease

**Conclusions:** Cardiomyopathy due to inborn errors of energy metabolism represents a rare cause of CT in adult population. Pathologists may play a role in unraveling the etiology, provided that a detailed diagnostic flowchart including histology and ancillary technique is followed.

**306 The Use of Artificial Intelligence in Diagnosing Acute Cellular Rejection in Cardiac Transplant Patients**

Matthew Glass<sup>1</sup>, Richard Davis<sup>1</sup>, David Dov<sup>2</sup>, Carolyn Glass<sup>3</sup>

<sup>1</sup>Duke University, Durham, NC, <sup>2</sup>Department of Electrical Engineering and Computer Science, Duke University, Durham, NC, <sup>3</sup>Duke University Medical Center, Durham, NC

**Disclosures:** Matthew Glass: None; Richard Davis: None; David Dov: None; Carolyn Glass: None

**Background:** Cardiac transplant patients must be on lifelong surveillance for the occurrence of rejection. Despite potent immunosuppressants, acute cellular rejection (ACR) remains an important problem and occurs when recipient T cells recognize donor antigens to cause myocyte destruction. Identifying ACR is usually a straightforward process for the trained pathologist, but distinguishing from other causes of T cell infiltration may be challenging in difficult cases. In such cases, interobserver variability even amongst the most experienced cardiac pathologists may exist. The aim of this study is to determine if a machine learning algorithm can reach acceptable performance of identifying ACR. This technology has recently been under robust investigation in cancer pathology but is less explored in non-neoplastic and transplant pathology. This is the first artificial intelligence (AI) algorithm to our knowledge, to diagnose ACR in cardiac transplant patients.

**Design:** All regions of ACR were annotated by a board-certified cardiac pathologist at a high-volume cardiac transplant center. Cases diagnosed as antibody-mediated rejection (AMR) were excluded. Annotations were extracted using the Openslide software and fed into a convolutional neural network which used the locked VGG16 base for transfer learning. After initially training our classifier, the last few layers of the convolutional base were unlocked and trained to fine tune the network. Keras was used for AI modeling and training. A three-layered annotation system was used to divide annotations into the 4 groups of interest.

**Results:** A total of 20,040 annotations (10,855 regions of ACR, 5002 healing injury, 423 Quilty lesions, 3760 normal) were completed from 200 hematoxylin and eosin slides scanned using a Leica Aperio AT2 digital whole slide scanner at 40X magnification. The AI algorithm distinguished ACR from normal cardiac tissue with 98-99% validation accuracy, ACR from Quilty lesion with 99% accuracy, and ACR from healing injury with 98% accuracy. The algorithm had the most difficulty distinguishing healing injury from normal cardiac tissue with a 93% validation accuracy.

**Conclusions:** With the rise of digitalized pathology, we provide evidence for the first time that a machine learning algorithm can be taught and validated to diagnose ACR. Multi-institutional studies to validate different grades of ACR as well as ACR with concomitant AMR pathology, are currently in progress.

**307 Primary Pericardial Pseudomyogenic Hemangioendothelioma**

John Gross<sup>1</sup>, Robert Ricciotti<sup>2</sup>, Jose Mantilla<sup>2</sup>, Yajuan Liu<sup>2</sup>, Ryan Morse<sup>2</sup>, Paul Swanson<sup>3</sup>, Haodong Xu<sup>2</sup>

<sup>1</sup>Mayo Clinic, Rochester, MN, <sup>2</sup>University of Washington, Seattle, WA, <sup>3</sup>University of Washington, Bainbridge Island, WA

**Disclosures:** John Gross: None; Robert Ricciotti: None; Jose Mantilla: None; Yajuan Liu: None; Ryan Morse: None; Paul Swanson: None; Haodong Xu: None

**Background:** Pseudomyogenic hemangioendothelioma (PMH) is a rare, indolent, endothelial neoplasm with distinct clinical and pathologic findings including recurrent *FOSB-SERPINE1* and *ACTB-FOSB* fusion genes. Within the last year, *ACTB-FOSB* gene fusion in PMH was reported at equal frequency (8 *FOSB-SERPINE1*, 7 *ACTB-FOSB*). PMH typically presents in young adult males as multifocal soft tissue or bone lesions, often involving multiple tissue planes and there are no cases of PMH primary to the pericardium in the literature. We describe our experience with primary pericardial PMH.

**Design:** One case of primary pericardial PMH was retrieved from our archives. Formalin-fixed and paraffin embedded tissue was utilized for all ancillary studies. RNA was extracted and used for anchored PCR/next generation sequencing (NGS) (Archer FusionPlex) according to standard protocol. Clinical and radiologic data were collected. An extensive literature search including all publicly available genomic databases was performed.

**Results:** A 34-year-old man presented with a clinical diagnosis of constrictive pericarditis. CT scan showed diffusely thickened pericardium (Figure 1A) leading to a pericardectomy and ultimately cardiac transplantation. Gross evaluation revealed dense, fibrous appearing, diffuse visceral pericardial thickening involving the explanted heart (Figure 1B). Histologically, the pericardial lesion was composed of sheets and intersecting fascicles of spindle cells with dense eosinophilic and vacuolated cytoplasm (1C, D) and invasion into endomyocardium. Immunohistochemistry showed positive staining for AE1/AE3, CD31 and ERG, while CD34 and desmin were negative (Figure 2A-D). Anchored PCR/NGS detected an *ACTB-FOSB* fusion gene supporting the diagnosis of PMH. The patient currently has no evidence of recurrent disease 4 months after cardiac transplant.

Figure 1 - 307

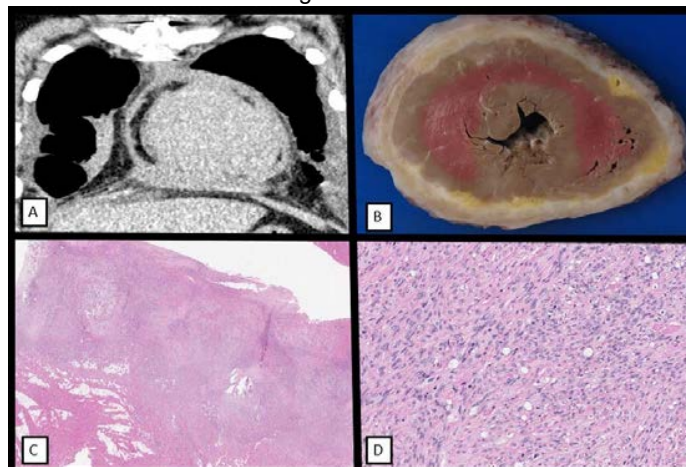
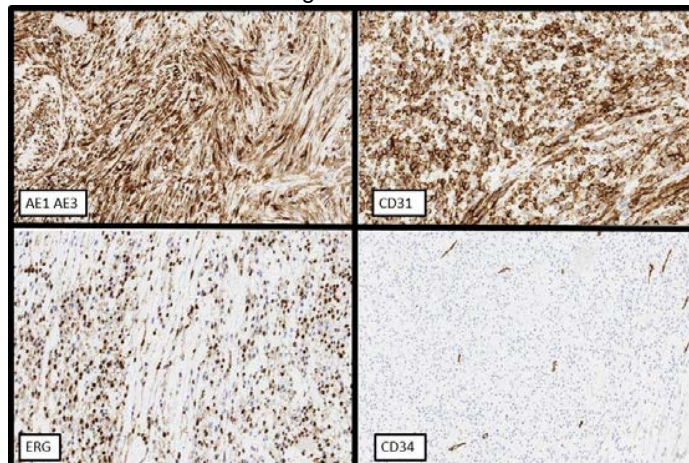


Figure 2 - 307



**Conclusions:** To our knowledge, this represents the first described example of a primary pericardial PMH and an additional example of an *ACTB-FOSB* translocation. Although rare, awareness of this entity in the differential diagnosis of spindle cell neoplasms or reactive myofibroblast proliferation of the pericardium and utilization of an immunohistochemical panel for vascular differentiation should allow for confident diagnosis in almost all instances.

### 308 Tissue Specific Induction of Nrg1 and ErbB4 during the Pathogenesis of Viral Myocarditis as Blood-Based Biomarkers for Diagnosis

Paul Hanson<sup>1</sup>, Al Rohet Hossain<sup>2</sup>, Gurpreet Singhera<sup>2</sup>, Bruce McManus<sup>3</sup>

<sup>1</sup>St. Paul's Hospital, Vancouver, BC, <sup>2</sup>St Paul Hospital/University of British Columbia, Vancouver, BC, <sup>3</sup>University of British Columbia and St. Paul's Hospital, Vancouver, BC

**Disclosures:** Paul Hanson: None; Al Rohet Hossain: None; Gurpreet Singhera: None

**Background:** Myocarditis, defined as inflammation of the myocardium, globally affects >3 million people annually. Heterogeneous histological findings and clinical presentation ranging from flu-like illness to acute cardiogenic shock make diagnosis exceedingly challenging. The current gold standard for diagnosis requires histological examination of invasive endomyocardial biopsies, which provides a sensitivity of <30% in independently published studies. Although there are many etiologies, viruses are the most prominent causes of myocarditis. Our studies have shown that the coxsackievirus B3 (CVB3), a common pathogen associated with viral myocarditis, manipulates the expression of Neuregulin 1 (Nrg1) and its ligand, receptor tyrosine-protein kinase, erbB4 during infection. Moreover, previous studies in other viruses have demonstrated preferential expression of the higher affinity Nrg1 $\beta$  versus the less potent Nrg1 $\alpha$  isoform. Here, we aim to analyze expression, tissue and isoform specificity of Nrg1 and ErbB4 in blood and heart tissue during the pathogenesis of viral myocarditis towards developing a non-invasive blood-based diagnostic assay via novel biomarkers.

**Design:** 4-week old male A/J mice were sham or CVB3 infected. Blood and tissue were harvested at time points corresponding to the acute, sub-acute and chronic phases of disease. Specimens were analyzed for mRNA and protein expression and sub-cellular localization using RT-qPCR, Western Blotting and confocal microscopy, respectively.

**Results:** Upregulation ( $p < 0.05$ ) of 65 kDa Nrg1 and 80 kDa ErbB4 protein fragments were observed in murine heart tissue at different phases of pathogenesis as compared non-infected controls. The observed upregulation was tissue specific and not observed in the infected pancreas or lung. In addition, ~35 kDa and ~26 kDa fragments of Nrg1 and ErbB4 respectively were detected in the plasma of infected mice absent in the non-infected controls. Nrg1 localized to the nuclear periphery while diffuse ErbB4 expression was observed during infection. mRNA levels of *Nrg1 $\beta$*  were significantly upregulated (~3-fold) at the acute phase (6-7 dpi), while the differences in expression of *Nrg1 $\alpha$*  were not significant.

**Conclusions:** Tissue specific upregulation and fragments detected in the plasma of both ErbB4 and Nrg1, with preferential expression of *Nrg1 $\beta$*  was observed as a result of CVB3 infection. These composite changes may be useful as biomarkers for developing a non-invasive blood-based diagnostic assay for viral myocarditis.

### 309 Incidence of Pathologic Antibody-Mediated Rejection in Right Ventricular Endomyocardial Biopsy Specimens Following Orthotopic Heart Transplantation – An Institution's Experience

Laura Lelenwa<sup>1</sup>, Kimberly Klein<sup>2</sup>, Sriram Nathan<sup>2</sup>, Carlos Manrique Neira<sup>3</sup>, Jerome Saltarelli<sup>3</sup>, Bihong Zhao<sup>4</sup>, L. Maximilian Buja<sup>5</sup>

<sup>1</sup>Houston, TX, <sup>2</sup>University of Texas Health Science Center at Houston, Houston, TX, <sup>3</sup>University of Texas Health Science Center at Houston McGovern Medical School, Houston, TX, <sup>4</sup>UTHealth, McGovern Medical School, Houston, TX, <sup>5</sup>The University of Texas Health Science Center at Houston, Houston, TX

**Disclosures:** Kimberly Klein: None; Sriram Nathan: None; Jerome Saltarelli: None; L. Maximilian Buja: None

**Background:** Antibody-mediated rejection (AMR) of cardiac allografts remains an important cause of morbidity and mortality among recipients of cardiac transplantation. Our aim was to perform a clinicopathological analysis of AMR, with or without acute cellular rejection (ACR), and to relate subcategories of AMR to clinical parameters in our cohort of orthotopic heart transplant (OHT) patients.

**Design:** A retrospective review of all post-OHT right ventricular endomyocardial biopsies (EMBs) performed at our institution over seven years was performed to determine the incidence of pathologic AMR (pAMR) with or without ACR. For each patient, EMB was performed weekly during the first month following OHT, and periodically thereafter. Examination for rejection was performed by immunofluorescence (IF) and light microscopy. We scored ACR and pAMR based on the ISHLT criteria. pAMR on post-OHT EMB specimens was classified as follows: transient pAMR (TpAMR) - only one biopsy with pAMR; intermediate pAMR (IpAMR) – 2 to 3 biopsies with pAMR; and persistent pAMR (PpAMR) – more than 3 biopsies with pAMR. At our institution, we routinely perform C4d staining by IF on all EMBs.

**Results:** During the study period, 265 patients underwent OHT at our institution. Of these, 244 (92.1%) developed some degree of ACR or pAMR (Figure 1). 48 patients (18%) developed pAMR diagnosed by histologic (H+) and/or immunologic (I+) findings. Of these, 20 (42%)



had ventricular assist devices (VADs) prior to OHT, 35 (72.9%) developed pAMR within 30 days, 2 (4.2%) developed pAMR between 31 and 60 days, and 11 (22.9%) developed pAMR more than 60 days post OHT (Figures 1 and 2; Table 1). Of the 48 patients with pAMR, 41 (85.4%) had both pAMR and ACR. Sub-classification as to duration of pAMR was 31.3% TpAMR, 41.7% IpAMR and 27% PpAMR. Of the 48 patients transplanted at our institution with pAMR, there were 4 deaths at <1, 1, 4, and 7 months post-OHT; 44 patients are alive with follow up ranging from 1 to 81 months (mean 40.2 months; median 41 months).

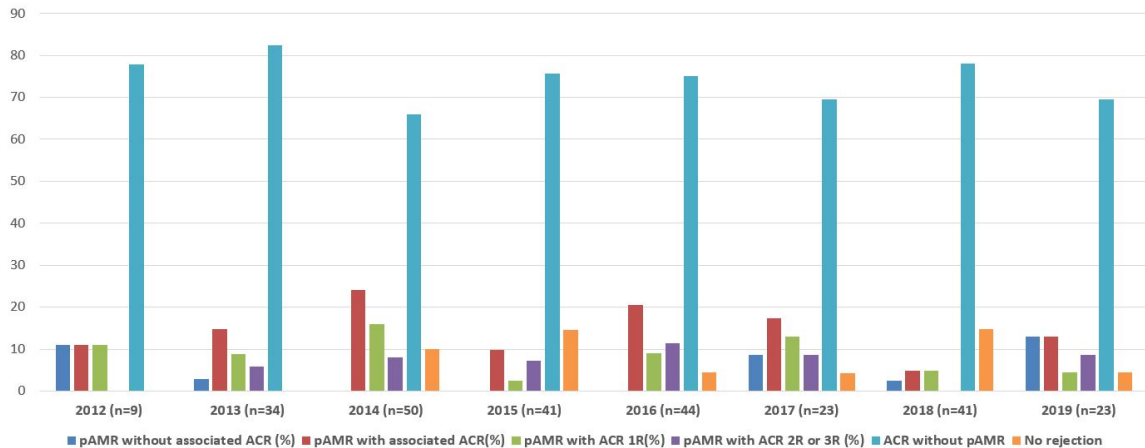
**Sub-classification of Pathologic Antibody-Mediated Rejection of Cardiac Allograft vis-à-vis Other Parameters**

	TpAMR	IpAMR	PpAMR
<b>Total</b>	15	20	13
<b>Onset post-OHT</b>			
≤ 30 days	8	15	12
31-60 days	1	0	1
> 60 days	6	5	0
<b>Additional findings</b>			
Associated ACR 1R	6	10	7
Associated ACR 2R – 3R	6	7	5
VAD prior to OHT	7	8	5
<b>Survival to date</b>	14 (93.3%)	17 (85%)	13 (100%)

pAMR – pathologic antibody-mediated rejection; TpAMR – transient pAMR; IpAMR – intermediate pAMR; PpAMR – persistent pAMR; OHT – orthotopic heart transplantation; ACR – acute cellular rejection; ACR 1R – grade 1 (mild) ACR; ACR 2R-3R – grade 2-3 (moderate to severe) ACR; VAD – cardiac ventricular assist device. Classification and grading of rejection on pathologic specimens was based on the 2004 consensus grading system of the International Society of Heart and Lung Transplantation (ISHLT).

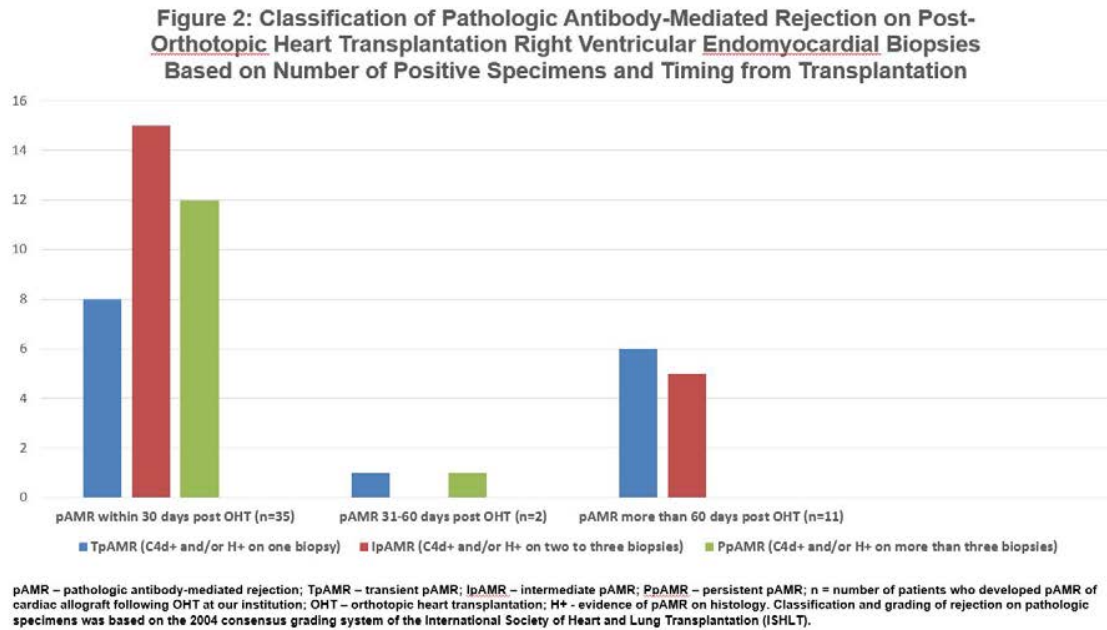
Figure 1 - 309

**Figure 1: Incidence of Rejection in Right Ventricular Endomyocardial Biopsies Following Orthotopic Heart Transplantation at our Institution from June 2012 through August 2019**



ACR - acute cellular rejection; ACR 1R – grade 1 (mild) ACR; ACR 2R-3R – grade 2-3 (moderate to severe) ACR; pAMR – pathologic antibody-mediated rejection; n = number of patients who underwent orthotopic heart transplantation and follow up cardiac biopsies at our institution. Classification and grading of rejection on pathologic specimens was based on the 2004 consensus grading system of the International Society of Heart and Lung Transplantation (ISHLT).

Figure 2 - 309



**Conclusions:** Thus, most patients who develop pAMR of cardiac allograft do so within the first 30 days following OHT and demonstrate multiple positive biopsies (IpAMR or PpAMR). At our institution, aggressive medical management including plasmapheresis and increased immunosuppression is instituted in the first 30 days post OHT. Further studies are planned to correlate duration of pAMR and clinical status, patient outcome, donor specific antibody levels, and timing of development of pAMR.

### 310 A Newer Indication for CRT? Low Myocardial Fibrosis on Histological Analysis Predict Cardiac Resynchronization Therapy Response

Li Li, Fuwai Hospital, Chinese Academy of Medical Sciences, Beijing, China

**Disclosures:** Li Li: None

**Background:** Cardiac resynchronization (CRT) is an effective treatment in addition to optimal drug therapy for heart failure with reduced ejection fraction. Unfortunately, the mechanisms underlying the response to CRT are poorly understood. Myocardial fibrosis has been identified as a determinant of the prognosis of cardiomyopathy progression. The aim of this study is assessing the relationship between response of CRT and myocardial fibrosis.

**Design:** Patients who underwent heart transplantation for heart failure were involved in this study. All the patients had underwent CRT implantation before heart transplantation. The recipient's heart was examined grossly and histologically and degree of myocardial fibrosis was evaluated. The time of CRT implantation and the invalid time of CRT were recorded. Then the relationship between the utility time of CRT and myocardial fibrosis was evaluated.

**Results:** Twenty-seven patients were included in this study. The average age was 54.0±10.0 years old and male to female was 23:4. Dilated cardiomyopathy was found in 19 patients, valvular heart disease in 2, myocarditis in 2, coronary heart disease in 1, arrhythmia right ventricular cardiomyopathy in 1, arrhythmia left ventricular cardiomyopathy in 1 and idiopathic atrial myopathy in 1. The average utility time of CRT was 881 days (0-3600 days). Twenty patients were good-responders to CRT with utility time of more than 180 days and 7 patients were poor-responders with utility time of less than 180 days. The average left ventricular and right ventricular myocardial fibrosis ratio in good-responder were lower significantly, compared to poor-responders (14.8±11.3% versus 31.7±31.0%, p<0.001 and 7.13 ±7.91% versus 17.1±29.4%, p=0.041). When compared left ventricular subendothelial and epicardial myocardial fibrosis ratio in two responders, epicardial myocardial fibrosis ratio was lower in good-responders (13.1±11.6% versus 23.0±25.0%, p=0.047). Interestingly, right ventricular subendothelial and epicardial myocardial fibrosis ratio were both lower in good-responders (7.9±8.8% versus 14.3±24.0%, p=0.027 and 4.4±5.7% versus 10.7±20.7%, p=0.018, respectively). Although the difference in interventricular septum fibrosis ratio in two groups was not significant, the fibrosis ratio of left ventricular side of interventricular septum was lower in good-responders (12.8±12.5% versus 22.7±34.5%, p=0.046).

**Conclusions:** The present findings show that a lower degree of left and right ventricular myocardial fibrosis is associated with a good response after CRT implantation. In left ventricle, epicardial fibrosis had a stronger relationship with CRT response. The fibrosis of left ventricular side of interventricular septum was also associated with CRT response. Myocardial fibrosis evaluation with MRI and endomyocardial biopsy before CRT implantation could help improve patient selection.

**311 Histopathologic Characterization of Hearts Status Post Radioablation for Refractory Ventricular Tachycardia**

Liang Lu<sup>1</sup>, Adam Lang<sup>2</sup>, Cuculich Phillip<sup>3</sup>, Stacey Rentschler<sup>3</sup>, Julie Schwarz<sup>3</sup>, Hannah Krigman<sup>4</sup>, Clifford Robinson<sup>3</sup>, Chieh-Yu Lin<sup>5</sup>  
<sup>1</sup>Washington University in St. Louis, St. Louis, MO, <sup>2</sup>Weldon Spring, MO, <sup>3</sup>Barnes Jewish Hospital/Washington University, St. Louis, MO, <sup>4</sup>Washington University School of Medicine, St. Louis, MO, <sup>5</sup>Washington University School of Medicine in St. Louis, St. Louis, MO

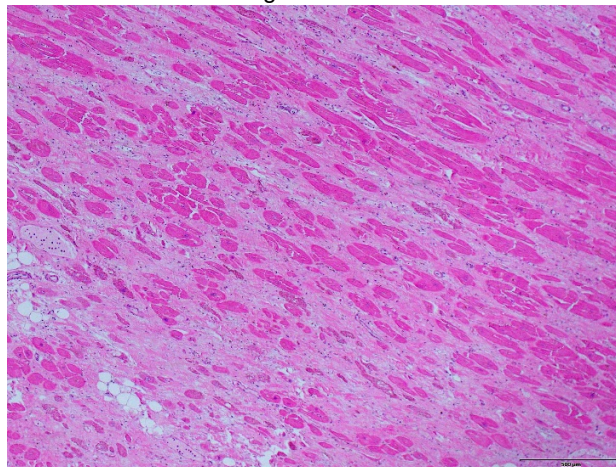
**Disclosures:** Liang Lu: None; Adam Lang: None; Cuculich Phillip: *Consultant*, Varian Medical Systems; *Consultant*, Medtronic; Stacey Rentschler: None; Julie Schwarz: *Grant or Research Support*, AACR/Bristol Meyers Squibb; *Grant or Research Support*, Goldman Sachs Philanthropy Fund; *Grant or Research Support*, Siteman Investment Program; Hannah Krigman: None; Clifford Robinson: None; Chieh-Yu Lin: None

**Background:** Recent clinical trials have demonstrated efficacy for stereotactic ablative radiotherapy (SABR) to treat ventricular tachycardia (VT) refractory to catheter ablation (CA). While multiple large animal studies have evaluated histological dose response to cardiac SABR, features after cardiac SABR in humans are largely unknown. In this study, we characterized the histopathologic features of SABR in the heart, in hope to further understand the mechanisms of this novel therapy.

**Design:** Institutional review board’s approval and patients’ informed consent were obtained. Four heart specimens were procured (three autopsies and one explant). Clinical information was obtained, including SABR site, time elapsed between SABR and tissue procurement, prior/subsequent treatment, and cause of death/transplant. Gross and microscopic examination was performed to assess the treatment effects (SABR and CA, if applicable). All patients were treated with SABR to a dose of 25 Gray in a single treatment.

**Results:** One case was examined 21 days after SABR. We observed only mild cardiomyocyte hypertrophy with minimally increased interstitial fibrosis in SABR area compared with background heart. The other 3 cases were examined more than 6 months after SABR (average:318 days). Gross examination of the SABR area showed patchy fibrosis without definite hemorrhage or transmural necrosis/fibrosis. Microscopic examination of the SABR area demonstrated ~50% of cardiomyocytes dropout. Compensatory cardiomyocyte hypertrophy and increased interstitial fibrosis were also noted, compared with the untargeted area (Figure 1). Mild interstitial inflammation and ectatic vessels were also present. The change encompassed ~ ½ thickness of the myocardium. We do not see evidence of recent/remote hemorrhage, reactive endothelial cells/endothelialitis, increased perivascular fibrosis, or accelerated atherosclerosis. In contrast, the areas of CA showed complete loss of cardiomyocytes, accounted for <1/3 thickness of myocardium.

Figure 1 - 311



**Conclusions:** We observed a unique histologic pattern in the hearts status post SABR, with partial loss of cardiomyocytes, interstitial fibrosis, and hypertrophic cardiomyocytes. With less cardiomyocyte loss/ fibrosis compared with CA, our findings suggest that a unique underlying mechanism other than fibrosis and reentry pathway blockage is accounted for the clinical efficacy of SABR in ventricular tachycardia.

**312 The Role of Therapeutic Plasma Exchange in Highly Sensitized Cardiac Patients**

Brenda Mai<sup>1</sup>, Yu Bai<sup>1</sup>, Castillo Brian<sup>1</sup>, Kimberly Klein<sup>2</sup>, Biswajit Kar<sup>1</sup>, Igor Gregoric<sup>1</sup>, Tint Hlaing<sup>1</sup>

<sup>1</sup>The University of Texas Health Science Center at Houston, Houston, TX, <sup>2</sup>University of Texas Health Science Center at Houston, Houston, TX

**Disclosures:** Brenda Mai: None; Yu Bai: None; Castillo Brian: None; Kimberly Klein: None; Biswajit Kar: None; Tint Hlaing: None

**Background:** Approximately 3,200 cardiac transplants are performed annually in the U.S. Sensitization, the development of circulating antibodies directed against human leukocyte antigen (HLA) proteins, poses a significant challenge to transplantation as there is an increased risk of organ rejection. The American Society for Apheresis (ASFA) has reported that therapeutic plasma exchange (TPE) has helped to avoid the intensive use of immunosuppressive and provide adjunctive therapy in desensitization and rejection protocol. High levels of class II antibodies have been reported to correlate with renal transplant rejection, however, no correlation has yet to be made of cardiac transplants.

**Design:** We retrospectively reviewed all desensitization cases from 2013 to 2016 at our institution. Pan-reactive antibodies (PRA) were identified before and after 10 TPE procedures and divided into class I and II in respect to their HLA antigen category. Antibody identification was determined using One Lambda Single Antigen Bead (SAB) Solid Phase (Luminex) assay. Antibody mediated rejection (AMR) and acute cellular rejection (ACR) were evaluated at numerous intervals post-transplant via right ventricular septum biopsies.

**Results:** 16 patients were treated with the desensitization protocol. Of these 16 patients, 9 patients underwent open heart transplant (OHT) and 2 underwent dual transplant with cardiac and renal (DDRT). Due to the deterioration of their clinical status, 6 patients underwent left ventricular assistant device (LVAD) placement. Included in the study were 10 men and 6 women with an average age of 53 (range: 30-68). An unpaired t test comparing the means of the pre-procedure and post-procedure PRAs revealed that there was a statistically significant reduction in Class I PRA titers (p-value: 0.003) whereas there was no statistical significant reduction in Class II PRA titers (p-value: 0.09). In addition, all patients that underwent desensitization protocol did not have evidence of AMR (Table).

No	Sex	Age	Type of Transplant	Pre Class I PRA	Pre Class II PRA	Post Class I PRA	Post Class II PRA	AMR	ACR
1	M	30	OHT	64	61	7	50	0	1R
2	M	58	OHT	88	39	0	0	0	2R
3	M	68	OHT	99	91	45	0	0	2R
4	M	59	OHT	99	0	59	0	0	1R
5	F	66	OHT	82	85	0	9	0	2R
6	M	66	OHT	83	0	0	4	0	1R
7	F	58	OHT	16	93	11	67	0	2R
8	F	37	OHT/DDRT	95	29	83	27	0	2R
9	M	41	OHT/DDRT	91	87	59	87	0	0

**Conclusions:** Our data suggests that TPE for desensitization protocol for cardiac transplants is only statistically significant for the elimination of class I HLA antibodies and not statistically significant for the reduction in class II HLA titers. In addition, the reduction of class I HLA titers may be positively correlated with decreased AMR. Therefore, patients with elevated class I HLA may benefit from the desensitization protocol for prevention of AMR, however, a larger scale investigation is required.

**313 Coronary Artery Calcium Score in Sudden Cardiac Deaths Cases in Postmortem Computed Tomography**

Katarzyna Michaud<sup>1</sup>, Virginie Magnin<sup>2</sup>, Tony Fracasso<sup>3</sup>, Silke Grabherr<sup>4</sup>

<sup>1</sup>Lausanne, Switzerland, <sup>2</sup>CURML (University Center of Legal Medicine Lausanne-Geneva), Lausanne, Vaud, Switzerland, <sup>3</sup>University Center of Legal Medicine, Lausanne and Geneva, Geneva, Switzerland, <sup>4</sup>University Center of Legal Medicine Lausanne-Geneva, Lausanne, Vaud, Switzerland

**Disclosures:** Katarzyna Michaud: None; Virginie Magnin: None; Tony Fracasso: None; Silke Grabherr: None

**Background:** Imaging methods have become essential in postmortem investigations, especially in forensic practice. Among them, postmortem computed tomography (PMCT) is the most widely accessible and the most frequently used. Sudden cardiac death (SCD) related to atherosclerotic coronary artery disease (CAD) is the most prevalent cause of death in western countries. In clinical practice, coronary artery calcium score (CACS) is considered as an independent predictor of CAD events, closely related to atherosclerotic burden and quantified radiologically by Agatston’s score (zero score- no evidence of CAD; 1-10 minimal CAD, 101-400 moderate CAD and >400 severe CAD). PMCT allows the visualization and quantification of coronary calcifications before the opening of the body.

**Design:** A retrospective evaluation of CACS in adults SCD cases related to CAD for which PMCT and CACS evaluations were available was performed. The autopsies were conducted in 2017 and 2018 according to international guidelines. Cases showing putrefaction, carbonization, traumatic lesions of the heart (not related to resuscitation attempts) and cases after percutaneous coronary revascularization procedures and coronary artery bypass grafting were excluded. The radiological examination was performed on a 64-row CT unit using a specific cardiac protocol. The CACS was calculated by using the software Smartscore 4.0.

**Results:** 36 cases were identified among 582 autopsies performed during the study period (29 men, 7 women; age 56.3±11.7). CACS was zero in 5 cases (5 men, 44.8±13.7), 11-100 in 8 cases (6 men, 2 women, 53.1±7.7), 101-400 in 13 cases (11 men, 2 women, 57.4±9.6) and more than 400 in 10 cases (9 men, 1 woman, 63.1±11.9). Acute coronary thrombosis was found in 28 cases (8 erosions, 20 ruptures) and cardiac tamponade in 3 cases.

**Conclusions:** In 36% of cases, postmortem CACS correspond to atherosclerotic burden considered clinically as zero or minimal. Therefore, SCD related to CAD can be missed on unenhanced PMCT. In postmortem imaging of coronary arteries, visualization of the lumen by angiographic methods is necessary. More postmortem imaging studies are necessary to deeper understand coronary calcifications and coronary plaques in SCD cases.

**314 Vulnerable Renal Artery with Aging Detected by Speed-of-Sound and Corresponding Histology**

Katsutoshi Miura<sup>1</sup>, Kanna Yamashita<sup>2</sup>

<sup>1</sup>Hamamatsu University School of Medicine, Hamamatsu, Shizuoka, Japan, <sup>2</sup>Department of Health Science, Hamamatsu University School of Medicine, Hamamatsu, Shizuoka, Japan

**Disclosures:** Katsutoshi Miura: None; Kanna Yamashita: None

**Background:** With aging, arteries alter to reveal mechanical weakness due to degeneration. Light microscopy is effective to follow morphological changes but difficult to evaluate mechanical properties. Because the speed-of-sound (SOS) through tissues increases with stiffness, mechanical weakness was evaluated by decreased SOS using scanning acoustic microscopy (SAM). This study aims to clarify the vulnerability of elderly renal artery (RA) by SAM with corresponding histology.

**Design:** Formalin-fixed-paraffin-embedded (FFPE) flat sections of renal arteries in 10 µm thickness from autopsy cases (n=36; age:16-101 y, mean 61.8 y, M=25, F=11) were scanned to calculate SOS values of each layer except calcified portions which were difficult to make flat surface and needed decalcification. We used 320 MHz transducer which resolution was 3.8 µm. SOS images were compared with the corresponding LM ones. SOS values of RA media were compared with those of ascending aorta. Moreover, SOS values after collagenase treatment on the sections were followed to detect sensitivity to protease.

**Results:** SOS values of media, internal and external elastic laminae had a significantly negative correlation with aging (Fig. 1) (p=0.003, 0.005, 1.1E-05, respectively). Corresponding histology displayed a reduction of smooth muscles and elastic fibers with collagen accumulation. Internal and external elastic laminae became thinner with fiber splitting. The both inside and outside diameters of media got longer and the inside/outside ratio decreased with aging, which meant that RA became expanded with constriction. All three layers especially tunica intima of RA became thicker with aging. There was a positive correlation of medial SOS between ascending aorta and RA (p=0.0055). By collagenase digestion, younger RA displayed a significant decrease in SOS (Fig. 2) while elderly RA showed no significant reduction.

Table 1. Comparison between SAM and LM observation

	SAM	LM
Observation procedure	No stainings necessary	Needs some stainings
Obtained images	Digital images	Analogue images
Color image changes	Adjustable based on the range of interest	Difficult to adjust images
Image analysis	Easy to compare SOS values	Needs conversion to digital data
Protease digestion	Easy to monitor after digestion	Difficult to detect alteration

Figure 1 - 314

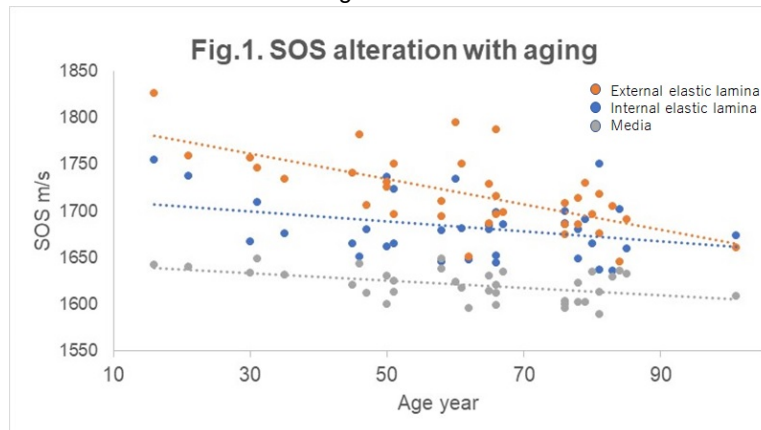
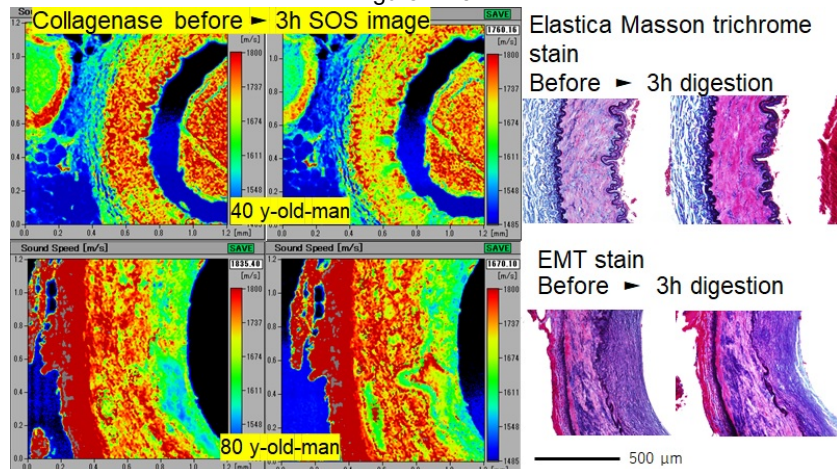


Figure 2 - 314



**Conclusions:** Decreased SOS values corresponded to the mechanical weakness of RA by aging, which correlated with degenerative histology. As a natural consequence of the mechanical weakness, medial layer of RA became dilated. Ascending aortae which showed similar degenerative changes have the same mechanism of mechanical weakness with aging as RA. Resistance to collagenase digestion in elderly may be due to some protein modifications. SAM observation has several advantages compared with LM one (Table 1).

### 315 Arrhythmogenic Cardiomyopathy: Autopsy Findings and Family Follow-up

Sarah Parsons<sup>1</sup>, Natalie Morgan<sup>1</sup>

<sup>1</sup>Victorian Institute of Forensic Medicine, Southbank, VIC, Australia

**Disclosures:** Sarah Parsons: None

**Background:** Arrhythmogenic cardiomyopathy (ACM) has large heterogeneity in its presentation, clinically, genetically and pathologically. It was originally described as a right ventricular disease however over time has progressed to be recognised as a bi-ventricular process. We will present a case series of 14 cases where a diagnosis of ACM had been made following sudden cardiac death (SCD).

**Design:** This study will review cases where ACM was given as the COD following SCD at our institution. Autopsy findings, family history and genetic testing results were reviewed.

**Results:** 14 cases were identified ranging in age between 22 and 51 years with 9 males and 5 females. All but one of the gross cardiovascular examinations were abnormal. Histologically all cases showed right and left ventricular involvement. 5 cases had moderate to severe coronary artery disease. All cases showed sub-epicardial fibrosis with fat infiltration predominately in left ventricle. There was no inflammation in 4 cases. Family histories were taken in all cases. In 3 cases SCD was identified in family members, 2 cases had a family history of congenital heart disease. 13 cases were followed-up at a cardiac genetics clinic. 3 cases had confirmed DSP mutations and 1 MYH7 class 4 mutation. The remaining 9 cases had variants of unknown significance (VUS) of these there was a clinical diagnosis of ACM in first degree relatives in 3.

**Conclusions:** Cases with a COD given as ACM at our Institute did not show isolated right ventricular involvement. The majority of cases had abnormalities on gross examination. Genetic diagnosis were made in 4 cases, 3 DSP mutations and one MYH7 class 4 mutation. Of the 9 cases with VUS's 3 had clinical diagnosis of ACM in family members. These cases highlight the importance for living family members of a diagnosis of ACM and follow-up of first degree family members.

**316 Sudden Cardiac Death in Hypertensive Heart Disease**

Joseph Westaby<sup>1</sup>, Mary Sheppard<sup>2</sup>

<sup>1</sup>London, United Kingdom, <sup>2</sup>Cardiovascular Sciences, London, England

**Disclosures:** Joseph Westaby: None

**Background:** Hypertensive heart disease refers to changes in myocardial structure and function that result from sustained hypertension. The relationship between hypertensive heart disease and sudden cardiac death is well established but there are few pathological studies. We examined the clinical and pathological features of hypertensive heart disease in sudden cardiac death victims.

**Design:** We investigated 5239 consecutive cases of sudden cardiac death referred to our national cardiovascular pathology centre between 1994 and 2018. Hearts were examined by an expert cardiac pathologist. Diagnostic criteria included increased heart weight and left ventricular wall thickness in the absence of other causes. Exclusion criteria were significant coronary artery disease and no premorbid diagnosis of hypertension.

**Results:** Of 75 sudden cardiac death cases due to hypertensive heart disease (age at death: 54±16years; 56% male), 56 (75%) reported no prior cardiac symptoms. Thirty-four (45%) recorded a BMI≥30. Four (5%) were labelled with hypertrophic cardiomyopathy in life, but lacked the diagnostic feature of myocyte disarray at autopsy. The mean heart weight was 563±153grams (males 636±140, females 470±114), with a maximal left ventricular wall thickness of 17.5±3.5mm. All hearts showed concentric hypertrophy. Fibrosis was present in 59 cases (81%) and was not associated with sex (p=0.31), BMI (p=0.17), or heart weight (p=0.48).

Demographic	Parameters	HHD (n=75)
Age	Mean±SD	54±16
	Range	18-85
Gender	Male	42(56%)
	Female	33(44%)
Ethnicity	White (British)	54(72%)
	White (Irish)	5(7%)
	White (other)	2(3%)
	Black (Caribbean)	2(3%)
	Black (African)	1(1%)
	Black (other)	1(1%)
	Unknown	7(9%)
Obesity		34(45%)
Diabetes		10(13%)
Chronic kidney disease		9(12%)
Cardiomyopathy/Hypertrophic Cardiomyopathy		6(8%)
Pregnancy		3(4%)
Died at rest or during sleep		60(80%)
Unknown		13(17%)
Died during emotional stress/assault		2(3%)
Breathlessness		17(23%)
Chest pain		4(5%)
Headache		3(4%)
Seizures		3(4%)
Palpitations		2(3%)
Vomiting/nausea		2(3%)
Syncope		1(1%)
Unknown Medication		49(65%)
Anti-hypertensive		21(28%)
None		5(7%)

Figure 1 - 316

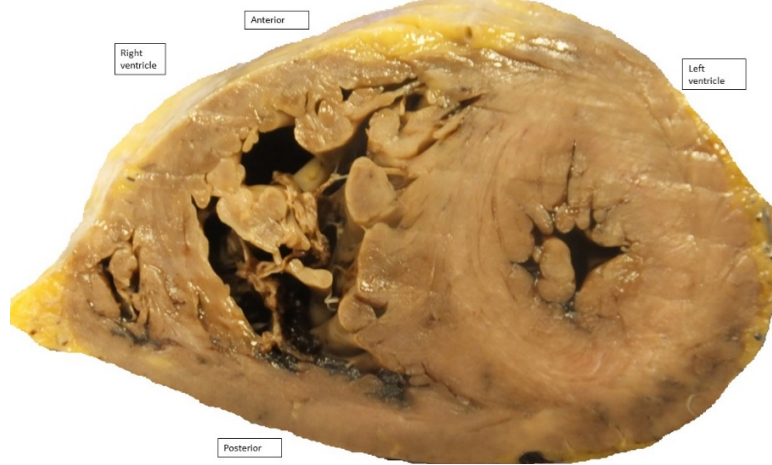
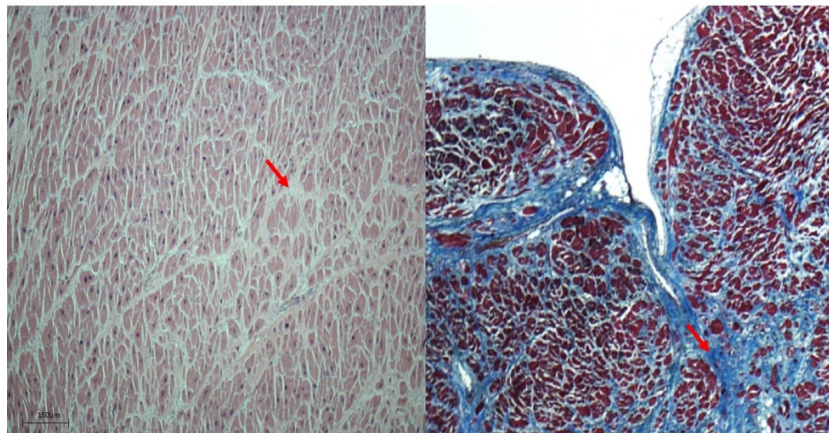


Figure 2 - 316



**Conclusions:** Most sudden deaths due to hypertensive heart disease occurred without prior cardiac symptoms so risk stratification is challenging. All cases exhibited concentric hypertrophy and myocardial fibrosis was frequently reported. Hypertensive heart disease should be excluded in those with left ventricular hypertrophy and hypertension prior to consideration of hypertrophic cardiomyopathy.